Compressible Flow Modeling Occurring in a Depressurization Process

V. Bruyere*[1], T. Paris[2], F. Viry[1], P. Namy[1]
[1]SIMTEC, 8 rue Duployé, Grenoble, 38100 France
[2]CEA DAM, Valduc, Is-sur-Tille, France
*Corresponding author: vincent.bruyere@simtecsolution.fr

Abstract: The depressurization process is the emptying of one tank to another one through a pipe network. In order to optimize the design of pipes and tanks, a good knowledge of the gas flow behavior is required. The modeling of compressible flows with a Mach number near 1 is quite challenging and simplifications are necessary to create an efficient numerical tool. Thus, a simple model is developed here, using COMSOL Multiphysics and the "Non-Isothermal Pipe Flow" interface. A theoretical validation is made by confrontation with analytical results. Then, using experimental results in multiple configurations, the model is adjusted to make it predictive.

Keywords: Compressible flow, Depressurization process, Gas discharge.

1. Introduction

The accurate modeling of compressible flows is still a challenge. In a pipe, oscillatory effects appear due to quick variations of the density when the Mach number is larger than 0.3 [1]. Still a macroscopic view of the phenomenon can be obtained thanks to many simplifications.

Here, the system is composed of two spherical reservoirs, the *container* (C) and the *receiver* (R), connected by a *pipe* (P) of constant section. They are all filled by a gas (Figure 1). The container is set to high-pressure, and is mechanically isolated of the rest by a *valve* (V). The system lies in an *environment* (E). The goal is to obtain a global view on the dynamic and the thermodynamic of the system at the opening of the valve, to get a better understanding of it.

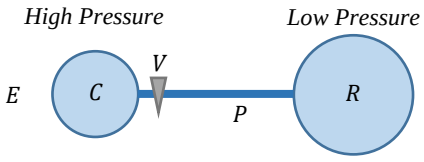

Figure 1. Overview of the system.

The model developed here is inspired by a simple approach proposed in [2]. First, a theoretical development is made. Then, a critical point of the implementation in COMSOL Multiphysics is discussed, illustrated by numerical issues. The validation of the model is achieved, based on theoretical results. Finally, it is adjusted using experimental data.

2. Modeling

A compressible flow is characterized by the movement variables and the thermodynamic quantities: the speed $u\,[m.s^{-1}]$, the density $\rho\,[kg.m^{-3}]$, the pressure $p\,[Pa]$ and the temperature $T\,[K]$. These quantities are linked by a system of 4 equations: the *mass*, *momentum* and *energy balances*, and the *constitutive equation*. In this work, the Reynolds number is high, of the order of 10^5, resulting in a turbulent flow. Plus, oscillatory effects appear when the Mach number is near 1. A global view is only necessary and the geometry is very simple. Hence, many hypotheses are proposed firstly. Then, the behavior of the gas within the system is described in each subsystem. Interface conditions are given to ensure the model consistency and to fulfill the second law of thermodynamics. Table 1 lists the parameters of the model.

Table 1. Parameters of the model

Entity	Parameter	Symbol [Unit]
Gas	Dyn. viscosity	$\mu\,[Pa.s]$
	Specific heat ratio	$\gamma\,[1]$
	Th. conductivity	$\lambda\,[W.m^{-1}.K^{-1}]$
	Molar mass	$M[kg.mol^{-1}]$
(P)	Length	$L\,[m]$
	Internal radius	$r\,[m]$
	Rugosity	$\varepsilon\,[m]$
(C)	Volume	$V^C\,[m^3]$
(R)	Volume	$V^R\,[m^3]$
(V)	Valve opening time	$\tau\,[s]$
(E)	Ext. temperature	$T^E\,[K]$
(C)	Initial pressure	$p_0^C\,[Pa]$
	Initial temperature	$T_0^C\,[K]$
$(P),(R)$	Initial pressure	$p_0\,[Pa]$
	Initial temperature	$T_0\,[K]$

Hypotheses

Due to the pipe dimensions, *i.e.* its diameter is negligible compared to its length, a 1-D approach is considered. Both of tanks are modeled in 0-D. To justify that, a set of hypotheses are given here, whose the most are adapted from [2].

The environment (E) is assumed to be isothermal in space and time. Since the size of the system is assumed to be negligible compared to the size of (E), and the duration of the process is less than 30 seconds, the heat diffusion in (E) is neglected.

The tanks (C) and (R) are simplified by points, since the interest of this study is to get the characteristic state of the gas at each time. In this case, the value of the variables is assumed to be spatially uniform. Since the diameter of the pipe is negligible compared to the size of the tanks, the velocity of the gas in these latter is assumed to be null. The gas is assumed to follow the ideal gas law. Thus, the specific heat capacities (c_v and c_p) are given under this hypothesis. Finally, the exchanges with (E) are approximated using the Nusselt number, as developed in [2], assuming that the natural convection prevails.

The pipe (P) is straight and of small constant section, allowing to model it by a segment. Thus, the movement variables and the thermodynamic quantities are approximated by their mean value on each section. During the process, the particles reach a high temperature and they are at high speed. In this case, their lifetime within the pipe is of the order of $1\,ms$. Thus, the flow is assumed adiabatic. Finally, as in the tanks, the gas is assumed to follow the ideal gas law.

These hypotheses require the introduction of several new variables. Each variable has a scalar value. This set of variables is given in Table 2.

Table 2. Variables of the model

Entity	Variable	Symbol [Unit]
(C)	Pressure	$p^C\ [Pa]$
	Temperature	$T^C\ [K]$
	Density	$\rho^C\ [kg.m^{-3}]$
(P)	Gas velocity	$u\ [m.s^{-1}]$
	Pressure	$p\ [Pa]$
	Temperature	$T\ [K]$
	Density	$\rho\ [kg.m^{-3}]$
(R)	Pressure	$p^R\ [Pa]$
	Temperature	$T^R\ [K]$
	Density	$\rho^R\ [kg.m^{-3}]$

In the following, $P1$ refers to the interface point $(C) \cap (P)$, $P2$ refers to $(P) \cap (R)$.

Fluid Behavior

In the pipe (P), the 4 equations describing a compressible flow stands as follows. Equations (1) (2) (3) refer to the *mass*, *momentum* and *energy balances*. Equation (4) is the *ideal gas law*.

$$\frac{\partial \rho}{\partial t} + \nabla(\rho u) = 0 \tag{1}$$

$$\rho\left(\frac{\partial u}{\partial t} + u\nabla u\right) = -\frac{\rho}{4r} f_D |u| u - \nabla p \tag{2}$$

$$\rho c_p \left(\frac{\partial T}{\partial t} + u\nabla T\right) = \nabla(\lambda \nabla T) + \frac{\rho}{4r} f_D |u| u^2 + \frac{\partial p}{\partial t} + u\nabla p \tag{3}$$

$$pM = \rho RT \tag{4}$$

In these equations, f_D is the *Darcy friction factor*, which describes the friction losses. It is given by the *Churchill's friction model* [3], which is accurate both in laminar and turbulent regimes, reached in the process. R is the gas constant. The operator ∇ refers to the spatial partial derivative $\frac{\partial}{\partial x}$.

In the tanks (C) and (R), the gas follows the *mass* and *energy balances*, and the *ideal gas law*. Being at a higher pressure than the rest of the system, (C) loses particles, and then energy, expressed as a gain of kinetic energy in the pipe. Symmetrically, (R) gains particles and energy. Both of them exchanges heat with the environment (E), using exchange coefficients h_W^C and h_W^R, expressed by the Nusselt number [2]. A refers to the section of the pipe. The coefficient S^C (resp. S^R) is the surface of the spherical volume V^C (resp. V^R). To do not overload the notations, in (C) (resp. (R)), without ambiguities, ρ, u and T designate their values at the extremities of the pipe $P1$ (resp. $P2$). In (C), (5) and (6) refer to the *mass* and *energy balances*, and (7), the *ideal gas law*.

$$V^C \frac{\partial \rho^C}{\partial t} = -\rho u A \tag{5}$$

$$\begin{gathered}\frac{\partial U^C}{\partial t} = -\rho u A\left(c_p T + \frac{u^2}{2}\right) + h_W^C S^C (T^E - T^C) \\ \frac{\partial U^C}{\partial t} = c_v V^C \frac{\partial(\rho^C T^C)}{\partial t}\end{gathered} \tag{6}$$

$$p^C M = \rho^C R T^C \tag{7}$$

In (R), (8) and (9) refer to the *mass* and *energy balances*, and (10), the *ideal gas law*.

$$V^R \frac{\partial \rho^R}{\partial t} = \rho u A \tag{8}$$

$$\begin{gathered}\frac{\partial U^R}{\partial t} = \rho u A\left(c_p T + \frac{u^2}{2}\right) + h_W^R S^R (T^E - T^R) \\ \frac{\partial U^R}{\partial t} = c_v V^R \frac{\partial(\rho^R T^R)}{\partial t}\end{gathered} \tag{9}$$

$$p^R M = \rho^R R T^R \tag{10}$$

Initial Conditions

At the beginning of the process, the valve is closed. In the pipe, the initial velocity, pressure and temperature are spatially uniform.

$$p^C(0) = p_0^C, T^C(0) = T_0^C \quad (10)$$

$$u(0) = 0, p(0) = p_0, T(0) = T_0 \quad (11)$$

$$p^R(0) = p_0, T^R(0) = T_0 \quad (12)$$

Interface Conditions

On $P1$ and $P2$, boundary conditions are necessary to couple the thermodynamic variables of the tanks and the pipe. It also defines well the flow within the pipe. These conditions are not trivial.

At the beginning of the process, during τ, the opening duration, there is a discontinuity between the pressure in (C) and on $P1$. Thus, a *temporal smoothing* is necessary, which transposes the idea that the pressure and the temperature of (C) are "transferred" to $P1$ (equations (13) and (14)).

$$p_{|P1} = (1-\theta)p_0 + \theta p^C \quad (13)$$

$$T_{|P1} = (1-\theta)T_0 + \theta T^C \quad (14)$$

In these equations, θ is a function depending only on time, such that $\theta(0) = 0$, $\theta(t) = 1$ for $t \geq \tau$, at least continuous.

During the process, the second law of thermodynamics imposes that the Mach number Ma within the pipe cannot exceed 1 since the section is constant. This critical state can only be reached on $P2$ [2]. For an ideal gas, the speed of sound is given by $c = \sqrt{\gamma \frac{R}{M} T}$, and the Mach number by $Ma = \frac{u}{c}$. When $Ma_{|P2}$ is beneath 1, the pressure on $P2$ is equal to the one in (R). At the critical state $Ma_{|P2} = 1$, shock waves arise in the receiver, and a critical pressure p^* is reached on $P2$, greater than the pressure in (R) (equation (15)). The gas is dumped in (R), that can be modeled by a heat outflow condition on $P2$ (equation (16)).

$$\begin{gathered} p_{|P2} = p^R \text{ and } Ma_{|P2} < 1 \\ \text{or} \\ p_{|P2} = p^* \text{ and } Ma_{|P2} = 1 \end{gathered} \quad (15)$$

$$\nabla T = 0 \quad (16)$$

3. Implementation with COMSOL Multiphysics

This system can be modeled in COMSOL Multiphysics. The *Non-Isothermal Pipe Flow* interface is used on a segment of length L to take into account the fluid flow. The exchanges with the tanks are implemented using the *Point ODE* interface on the extremities. The *Events* interface is used to treat the critical state.

Numerical Aspects of the Critical State

The equation (15) implies a change of the boundary condition on the pressure on $P2$ during the process. In order to treat that case, an equation is used to choose the out pressure according to the sonic regime on $P2$. Because of the *floating-point inaccuracies* and the error made during the computation, the case $Ma_{|P2} = 1$ is not reachable numerically. Using a threshold on $Ma_{|P2}$ to detect this case is not sufficient, since it can cause a wide discontinuity on the velocity and the pressure on $P2$, and it makes impossible the return to $Ma < 1$. A cycle between both sonic states exists, and can be modeled by a *Moore machine* (Figure 2, in black). Thanks to the notion of *sonic state*, this automaton can be modified using well-chosen thresholds, in order to be usable numerically. They are chosen such that the conditions (a) and (d) cannot be satisfied at the same time (resp. (b) and (c)) (Figure 2, in red).

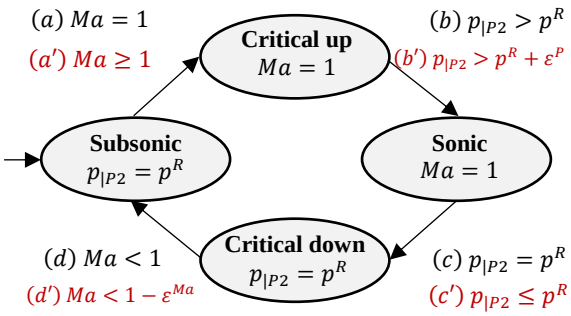

Figure 2. Cycles of the critical condition.
The boundary condition is given for each state in each bubble. Next to the arrows are the conditions of transition between each state. The conditions in continuous time are in black, whereas the conditions in discrete time for numerical purposes are in red.

In COMSOL Multiphysics, the *Events* interface makes it possible to transpose this automaton. This interface needs to use a temporal solver. The advantage is that, during the computations, when a transition is almost satisfied, the solver takes small time steps in order to be as accurate as possible.

Space and Time Discretization

To be confident with the results, it is necessary to choose adapted steps of discretization in space and time. A study of sensitivity to the mesh shows that it is sufficient to mesh the segment by a uniform distribution of at least 1000 nodes. A coarser mesh induces a loss of mass during the process, due to

discretization errors. The time discretization needs more accuracy. Since the critical condition is reached very quickly, an initial step of at most $10^{-7}s$ is a good choice. When $Ma_{|P2}$ returns to less than 1, the gas is less agitated and the step chosen automatically by COMSOL Multiphysics is sufficient.

4. Theoretical Validation

In order to make sure that the model is able to simulate accurately the process, a validation step is necessary. First, a numerical validation is performed, by verifying a few necessary conditions on the solution, often given by physical balances. Then, a comparison with analytical results is also made in a simplified case, to check the consistency of the model with the theory.

Checking with Balances

To avoid rapidly large inconsistencies with the theory, checking physical balances is advocated. For example, a first checking of the consistency of a flow can be made using a mass flow rate balance (equation (17)). In the same way, the respect of the ideal gas law in the pipe can be checked (equation (18)).

$$A\left(\rho_{|P1}u_{|P1} - \rho_{|P2}u_{|P2} - \int_P \frac{\partial \rho}{\partial t}dx\right) = 0 \qquad (17)$$

$$pM - \rho RT = 0 \qquad (18)$$

The only difficulty is to appreciate the result. These equations will never be respected, due to the numerical errors. Informally, to use it as a quick way to verify if there is an inconsistency, it is sufficient to check that these quantities are close to 0, *e.g.* the absolute value is less than 10^{-3}.

Comparison with Analytical Results

In order to check the respect of the critical condition and to increase the confidence with the model, a comparison with analytical results in a simplified case is made here. Only the flow within the pipe is considered. In the case of a steady flow without friction losses, the value at the extremity of the pipe for p, T, ρ and q_m, the mass flow rate, are known under the critical condition [4]. To attain quickly $Ma_{|P2} = 1$, a convergent pipe is considered, ending by a col, *i.e.* A is a function of x. The *mass*, *momentum* and *energy balances* are rewritten as follows, completed by the *ideal gas law* (equations (19) (20) (21) (22)).

$$\nabla(A\rho u) = 0 \qquad (19)$$

$$\rho u \nabla u = -\nabla p \qquad (20)$$

$$A\rho c_p u \nabla T = \nabla(A\lambda \nabla T) + Au\nabla p \qquad (21)$$

$$pM = \rho RT \qquad (22)$$

The boundary conditions are chosen such that the critical condition is reached at the end extremity of the pipe. Thus, a high pressure is imposed in $P1$ (*e.g.* 300 bar) and the velocity in $P2$ is chosen such that $Ma_{|P2} = 1$. Under these conditions, the critical values are the following [4] (equations (23) (24) (25) (26)).

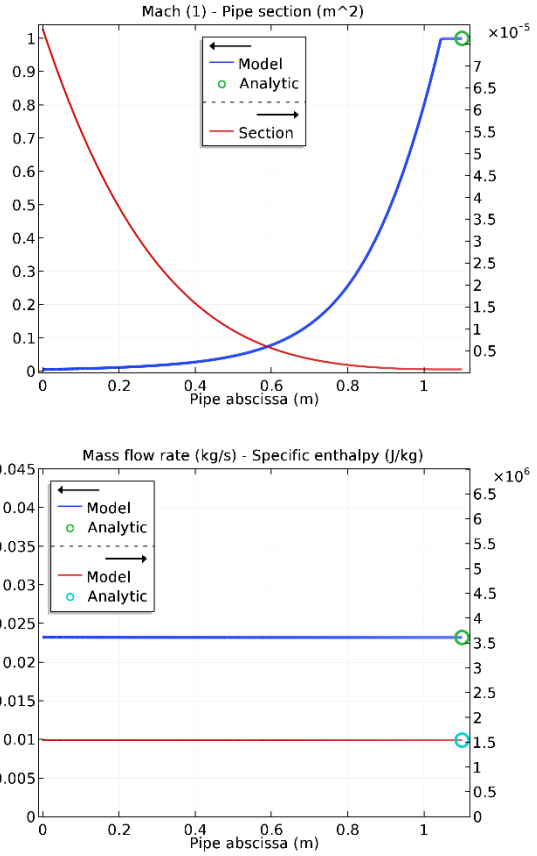

Figure 3. Mach number and A (top), and mass flow rate and enthalpy conservation (bottom) along the pipe.

Figure 3 gives confidence in the model. The values for the Mach number, the pressure, the temperature, the density and the mass flow rate at the extremity of the pipe are the same than those predicted by the theory. Plus, the mass flow rate and the enthalpy are conserved.

$$p_{|P2} = p_{|P1}\left(\frac{2}{\gamma+1}\right)^{\frac{\gamma}{\gamma-1}} \quad (23)$$

$$T_{|P2} = T_{|P1}\frac{2}{\gamma+1} \quad (24)$$

$$\rho_{|P2} = \rho_{|P1}\left(\frac{2}{\gamma+1}\right)^{\frac{1}{\gamma-1}} \quad (25)$$

$$q_m = \left[\frac{M}{R}\left(\frac{2}{\gamma+1}\right)^{\frac{1}{\gamma-1}}\sqrt{\frac{2\gamma R}{M(\gamma+1)}}\right]\frac{p_{|P1}}{\sqrt{T_{|P1}}}A_{|P2} \quad (26)$$

5. Adjustment with Experimental Results

The purpose of this model is to forecast the gas behavior within the pipe and the tanks. Here, the results of the model are compared with experimental data, in order to adjust it. In these experiments, a gas is put at high pressure in (C), whereas (P) and (R) are put under vacuum. The data come from two batches of experiments including those from [2] prefixed by $SCh96$. Different gases and pressures have been used. Table 3 gathers the gas types and the initial pressures in (C) and (P) and (R) for each experiment.

Table 3. Condition of the experiments

Experiment	Gas	p_0^C [bar]	p_0 [bar]
$SCh96\ III$	Helium (^{4}He)	319	0.08
$SCh96\ XI$	Deuterium (D_2)	308	0.11
$E1$	Argon (Ar)	162	0.01
$E2$	Helium (^{4}He)	135	0.5
$E3$	Helium (^{4}He)	60	0.4

Adjustments of the Equilibrium Pressure

A first step consists in the comparison of the experimental and the model pressures in the tanks. Globally, the behavior of the pressure is captured by the model, *i.e.* the trend of the model fit the trend of the experiments (Figure 4, Figure 5). However, a shift on the pressure in (R) is present on each experiment $E1$, $E2$, $E3$. In fact, the quantity of gas in (C), *i.e.* its mass, seems to be underestimated. We could explain this by an inaccurate measure of the temperature, particularly the initial one. In reality, in the experiments $E1$, $E2$, $E3$, a first discharge occurs from (C) to an auxiliary pipe network (not shown here), before the discharge studied here. Thus, (C) is not initially at a thermodynamic equilibrium, contrary to (R). Since the heat diffusion to the sensor is a slow process, the measured temperature is smoothened and delayed, resulting in an overestimation of our initial temperature in (C).

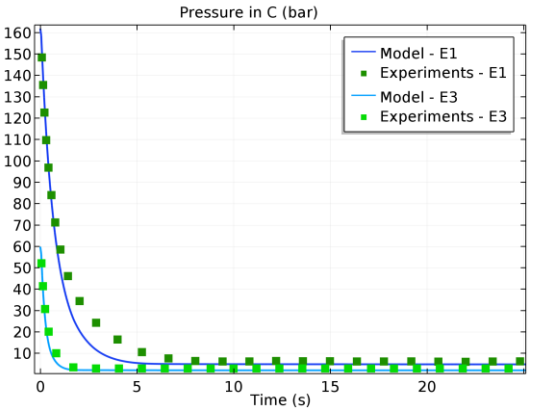

Figure 4. Pressure in the container, $E1$ and $E3$.

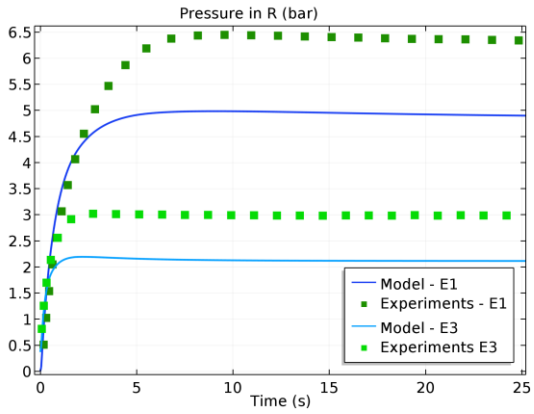

Figure 5. Pressure in the receiver, $E1$ and $E3$.

The system reaches an equilibrium state when the time tends to infinity. We assumed that the temperature in the environment is spatially and temporally uniform, *i.e.* the equilibrium temperature is T^E. The experimental results make it possible to estimate the equilibrium pressure, and then the equilibrium density too. The mass of gas within the system can be deduced. Thus, the initial temperature in (C) can be deduced applying the constitutive equation. Figure 6 and Figure 7 show the results using an initial temperature consistent with the equilibrium state. The trend of the transient state differs a bit of the experiments at the end of the discharge. A possible reason is an underestimation of the thermal exchanges between the tanks and the environment. With this correction, the gas temperatures decreases rapidly into very low values (of the order of $120\,K$), which induces a fast decrease of the pressure. The differences between the simulated and the real temperatures are discussed more precisely in the following part.

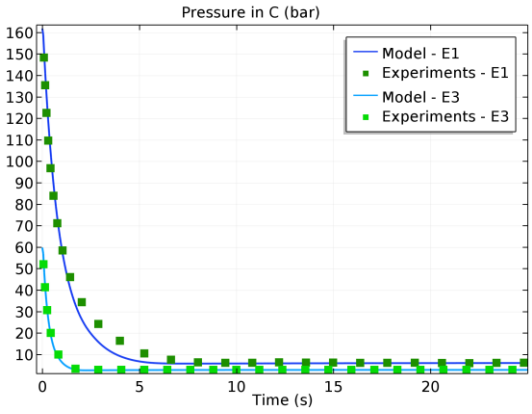

Figure 6. Pressure in the container, E1 and E3, with the correction of the initial temperature.

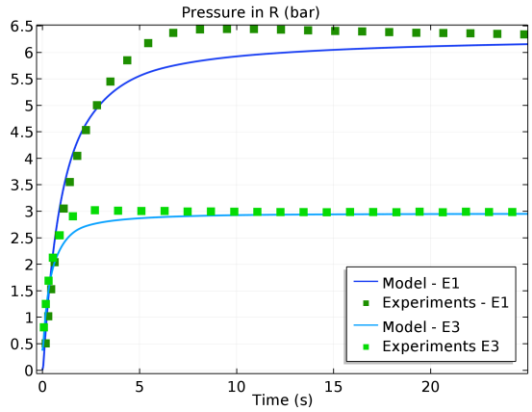

Figure 7. Pressure in the receiver, E1 and E3, with the correction of the initial temperature.

Adjustments of the Temperature

Under our hypotheses, the model does not validate the measured temperatures of $E1$, $E2$ and $E3$. Thus, we propose here to compare the temperatures predicted by the model with the measured temperatures of the experiments $SCh96\,III$ and $SCh96\,XI$ from [2], where a correction of the measurements is proposed, taking into account the process of heat diffusion in the sensor. The trend of the transient state in (C) has been captured by the model during the first seconds of the process, but the results are inaccurate (Figure 8, Figure 9). It is encouraging, since many simplifications have been made on the thermal exchanges.

In (R), it is much more complicated. The natural convection was assumed to prevail, but the forced convection generated by the sonic jet of gas is not negligible [2]. A strong hypothesis of the model was the uniformity of the temperature in the tanks, which is certainly false during the discharge. A correction of the estimation of the Nusselt number is proposed in [2]. However, in both conditions, the model seems to do not make enough exchanges of heat between (R) and (E), resulting in thermal aspects completely driven by the forced convection (Figure 10).

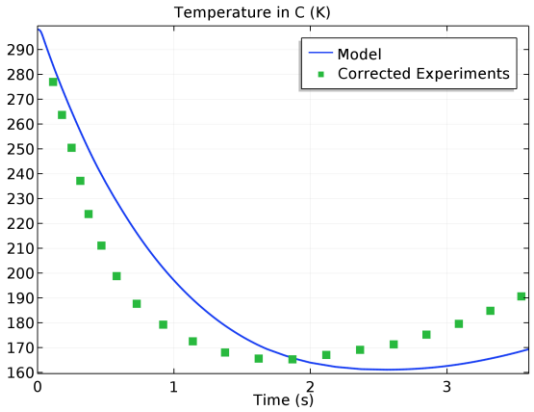

Figure 8. Temperature in the container, $SCh96\,III$.

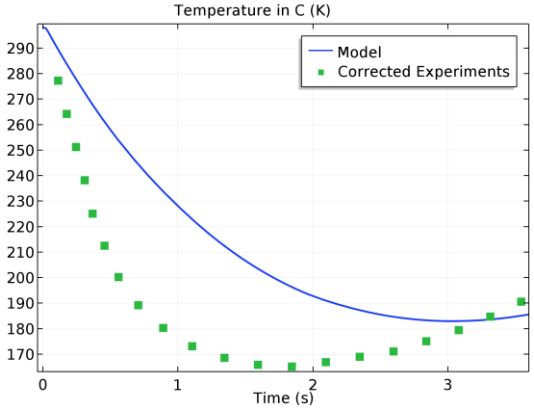

Figure 9. Temperature in the container, $SCh96\,XI$.

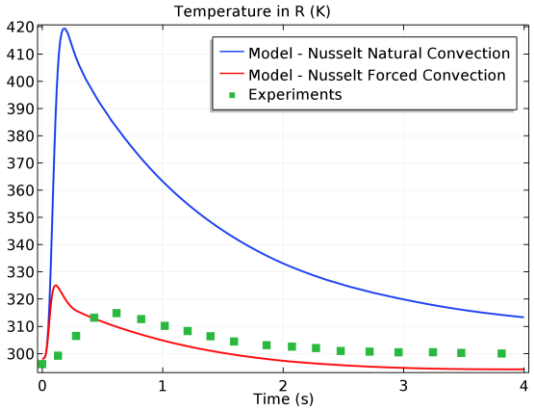

Figure 10. Temperature in the receiver, $SCh96\,XI$.

6. Conclusions

Here, we developed a model of the flow of a gas within a pipe during a discharge, coupling the flow and the thermal exchanges in a 1-D approach. We have validated the model on the theoretical point of

view in a simplified case, and we have compared its predictions with experimental results. The results are promising. Under the correction of the initial temperature in the container to get consistency with the equilibrium state of the system, the model gives satisfactory values for the pressure in the tanks. Thus, it gives confidence in this 1-D approach that uses the ideal gas law.

The simplification of the thermal exchanges in the tanks is one of the limits of the model. The uniformity of the temperature is too restrictive, but dropping it will result in breaking the 0-D approach. To get a better understanding of the heat transfers in the receiver tank, it is conceivable to study more precisely it separately in 2-D or 3-D. Such a study could allow to change the estimation of the thermal exchange terms.

References

[1] COMSOL, The COMSOL User's Guide, 2012, p. 674.

[2] S. Charton, V. Blet and J. P. Corriou, A Simplified Model for Real Gas Expansion Between Two Reservoirs Connected by a Thin Tube, vol. 51, 1996, pp. 295-308.

[3] S. W. Churchill, Friction factor equation spans all fluid-flow regimes, 1977, pp. 91-92.

[4] A. Lallemand, Ecoulements monodimensionnels des fluides compressibles, *Techniques de l'ingénieur*, 2014.